RSC Advances

ROYAL SOCIETY OF CHEMISTRY

www.rsc.org/advances

Journal Name

ARTICLE

Flexible and Mechanically-stable MIL-101(Cr)@PFs for Efficient Benzene Vapor and CO_2 Adsorption

Zhenyu Zhou, [a] Baihua Cheng , [a] Chen Ma , [a] Feng Xu, [b] Jing Xiao, [*b] Qinbin Xia , [b] and Zhong Li [*a]

Received 00th January 20xx,
Accepted 00th January 20xx

DOI: 10.1039/x0xx00000x

www.rsc.org/

Novel composites MIL-101(Cr)@PFs were successfully prepared by immobilizing MIL-101(Cr) crystals onto the 100% virgin pulp fibers(PFs), and then characterized by N_2 adsorption, X-ray diffraction (XRD), scanning electron microscopy(SEM), Fourier transform infrared spectroscopy (FT-IR) and thermal analysis. The adsorption isotherms of CO_2 and benzene vapor on MIL-101(Cr)@PFs were measured by a volumetric method. Mechanical stability of sheet MIL-101(Cr)@PFs were tested on an oscillator with adjustable oscillation frequency of 2 and 4 Hz. Results showed that the as-synthesized MIL-101(Cr)@PFs demonstrated similar gas uptake to the parent MIL-101(Cr) as well as excellent stability. The surface area of MIL-101(Cr)@PFs increased with the loaded amount of MIL-101(Cr). The uptakes of 67MIL-101(Cr)@PF for CO_2 and benzene vapor reached 2.13 mmol/g and 10.29 mmol/g at 298 K respectively, close to those of unit mass of MIL-101(Cr) loaded on the pulp fibers, suggesting high utilization efficiency of MIL-101(Cr) after casting on PFs. MIL-101(Cr)@PFs prepared in this work were flexible. 50MIL-101(Cr)@PFs can be distorted up to 360° without damage. Importantly, mass retention rate of MIL-101(Cr)@PFs maintained up to 99% after vibration of 120 minutes at 2HZ or 4HZ, implying that MIL-101(Cr) crystals had been anchored on pulp fibers stably. It could be expected that the sheet MIL-101(Cr)@PFs would become a promising adsorption material for gas adsorption and purification in practical applications.

1. Introduction

Metal Organic Frameworks (MOFs), as a family of emerging porous materials, have attracted the increasing attention of scientists worldwide during the last two decades.[1, 2] The huge surface area and pore volume, controllable pore size distribution and adjustable surface properties of MOFs[3-5] enable it to play a crucial role in many functional applications, such as catalysis,[6, 7] hydrogen storage,[8, 9] CO_2 capture[10-12] and harmful gas adsorption.[3, 13]

Recently, increasing attentions are focused on detrimental environmental and health effects resulting from the emission of Volatile organic compounds (VOCs) and CO_2. Adsorption is generally considered to be a fast, safe, and economical approach to remove VOCs and CO_2. Thus, the use of adsorbents with high adsorption capacity would be an ideal solution for the efficient removal of VOCs and CO_2. However, it was reported that the conventional adsorbents, such as activated carbon,[14, 15] zeolite,[16, 17] silica gel[18] showed low adsorption capacities towards VOCs and CO_2, and the MOFs were thought as promising adsorption materials for VOCs and CO_2 capture and separation since they have much higher adsorption capacity towards VOCs and CO_2 compared to conventional adsorbents. Millward and Yaghi[19] reported that the CO_2 adsorption capacity of MOF-177 reached 33.5 mmol/g at 298 K and 35 bar. As one of the most stable MOFs, MIL-101(Cr) achieved a high CO_2 adsorption capacity of 23 mmol/g at 298 K and 30 bar reported by Li..[20] In addition, Zhao.[21] reported that benzene adsorption capacity of HKUST-1 at 25 mbar and 298 K was about 10 mmol/g. Jeremias.[22] reported that methanol adsorption capacities of HKUST-1 and MIL-101(Cr) were about 0.55 and 1.15 g/g at 298 K (p/p_0=0.8), respectively. Furthermore, in order to enhance adsorption performance of MOFs, some MOFs-based composites were invented. For example, Sun[3] prepared the composites (MIL-101@GO) of MIL-101 and graphite oxide, and reported that MIL-101@GO exhibited the maximum n-hexane uptake of 1042.1 mg/g at 298 K, which increased by 93% in comparison with that of the MIL-101, and was much higher than those of the conventional activated carbons and the zeolites. Zhou[4, 23] synthesized the composites GrO@MIL-101 of MIL-101 and graphene oxide, and reported that GrO@MIL-101 had higher high acetone adsorption capacity and CO2 adsorption capacity as well as CO_2/CH_4 selectivity compared to parent MIL-101.

In spite of the excellent uptake capacities of MOFs or MOFs-based composites for VOCs and CO_2, up to now, no practical application of MOFs has been reported yet. Actually, it is difficult to apply directly MOFs in practical application because MOFs are powders. If the powders of MOFs were directly exposed to air flow, they would be blown away. If the powders of MOFs were directly filled in a fixed bed, it would cause a high bed pressure drop due to high adsorbent-packing density when gas stream flows through the bed. It is considered that if MOFs could not be put in use in near future, its development would be hindered. From viewpoint of application, MOFs are still in an immature state.[7, 24, 25] In order to solve this problem, it is especially important to study the forming of MOFs powders into different shapes，such as spherical, cellular, fiber sheet, and fiber cloth. Therefore, the immobilization of MOFs powders onto structured supports is of great importance, not only for gas adsorption but also for other applications like catalysis,[7] textile industry,[26] photocatalytic purposes[27] and so on.

However, only little efforts have been devoted to the immobilization of MOFs onto structured supports.[7, 28] There were few reports about the immobilization and molding of MOFs crystals on various modified surfaces. For example, Fernandez[7] immobilized MIL-101(Cr) on a monolithic structure via the secondary seeded growth method, and the MIL-101(Cr) monolith not only presented long-term stability but also exhibited similar catalytic performance to tetralin with respect to that of the powders. Marcia[29] grew HKUST-1 on cotton with carboxyl groups for the fabrication of functionalized fibers, and confirmed a strong chemical interaction of HKUST-1 with the carboxymethylated cellulose fibers. However, no adsorption and mechanical property were reported. Rose[26] reported the immobilization of MIL-100(Fe) and HKUST-1 crystals by electrospinning on composite polymeric fibers, and the high loadings of MOF up to 80 wt% in the polymeric fibers could be achieved.

To the best of our knowledge, so far, there is no report that natural pulp fiber (PF) has been used to prepare sheet MOFs@PFs adsorbents for gas adsorption. Among all substrates, the PF is considered to be an excellent choice because it is economical, highly flexible and easily molded.[25] Furthermore, the PF itself contains some oxygenic groups, such as carboxyl groups, which would be conductive to the formation coordination bonds between surface carboxyl groups of PF and some mental ions of MOFs.[30]

Herein, we prepared the composites MIL-101(Cr)@PFs of MIL-101(Cr) and the pulp fibers for the first time, then tested their flexible and mechanical stability, and examined their adsorption performances towards benzene and CO_2. The effects of MIL-101(Cr) loadings of the sheet composites on their textural structures, adsorption performances for VOCs and CO_2 and mechanical stability of MIL-101(Cr)@PFs were discussed, and then reported here.

2. Experimental section

2.1. Materials

Terephthalic aicd (H_2BDC, 99%, A.R.) was purchased from Alfa Chemicals. Chromium nitrate nonahydrate($Cr(NO_3)_3{\cdot}9H_2O$, 99%, A.R.) was got from Tianjin Fuchen Chemicals Co. Ltd. (Tianjin, China). N,-N dimethylmethanamide (DMF, 99.5%) , ethanol (99.7%) and hydrogen peroxide solution(H_2O_2, 30%) were provided by Guangzhou Guanghua Sci-Tech Co. Ltd. Hydrofluoric acid (40%) and benzene (99.5%) were purchased from Guangzhou Chemical Reagent Factory. 100% virgin pulp paper was purchased from Vinda Paper Company.

2.2. Oxidation treatment on virgin pulp fibers

Before as matrix material, 100% virgin pulp fibers needed to be treated by hydrogen peroxide solution to increase surface oxygenic functional groups.[31] The procedures were as follows: first, the 100% virgin pulp papers were immersed in distilled water and stirred for 1-2 h,then filtrated. Second, the virgin pulp fibers and hydrogen peroxide solution(3 mol/l, 30 ml) were mixed in the teflon autoclave reactor and then the reactor was heated at 358 K for 8-12 h. Then, the reactor was cooled down to the ambient temperature gradually. After that, the pulp fibers were washed several times by sufficient distilled water and then dried at 308 K for use.

2.3. Preparation of composite MIL-101(Cr)@PFs

Synthesis of MIL-101(Cr) was performed according to the procedures described in the literature.[13] Chromium nitrate, terephthalic acid, distilled water and HF solution were used to prepare MIL-101(Cr). Before preparation of MIL-101(Cr)@PFs, the MIL-101(Cr) was dried at 373 K and then evacuated at 423 K for 12 h in a vacuum condition.

Sheet MIL-101(Cr)@PFs were prepared by a deposition method. Fig.1 presents the flow chart of preparation of the sheet composites MIL-101(Cr)@PFs. Preparation procedure was as follows: first, the pulp fibers (0.3 g) treated with hydrogen peroxide solution were added in distilled water and stirred at room temperature for 8-12 h. Thus, pulp suspension was obtained. Second, MIL-101(Cr) crystal powers (0.1, 0.2, 0.3, or 0.6 g) were mixed in the pulp suspension and stirred at 313 K for 4 h. After that, the resulting mixture was filtered using G_4 funnel, dried at 308 K and then activated at 423 K for 12 h under vacuum. Finally, sheet MIL-101(Cr)@PFs were obtained. The contents of MIL-101(Cr) crystals loaded on MIL-101(Cr)@PFs were 25%, 40%, 50% and 67%, respectively. Correspondingly, MIL-101(Cr)@PFs were denoted as 25MIL-101(Cr)@PFs, 40MIL-101(Cr)@PFs, 50MIL-101(Cr)@PFs, and 67MIL-101(Cr)@PFs, respectively.

2.4. Adsorbent characterizations

Nitrogen adsorption isotherms were measured at 77 K on Micromeritics' Accelerated Surface Area and Porosimetry Analyzer 2010 (ASAP 2010) equipped with commercial software of calculation and analysis. The pore textural properties such as specific Langmuir surface area, Brunauer–Emmett–Teller (BET) surface area were obtained by analyzing the N_2 adsorption isotherms. The pressure ranges used for the BET surface area calculations were $0.05 < P/P_0 < 0.25$ (Based on the three consistency criteria[32, 33]). Pore volume data and pore size distribution calculation also were provided by ASAP 2020 equipped with the software based on Density Functional Theory (DFT). The samples were outgassed at 423 K for 8 h before each measurement.

Powder X-ray diffraction (PXRD) data were recorded on a Bruker D8 Advance X-ray diffractometer with Cu Kα radiation at room temperature with a scan speed of 2°/min and a step length of

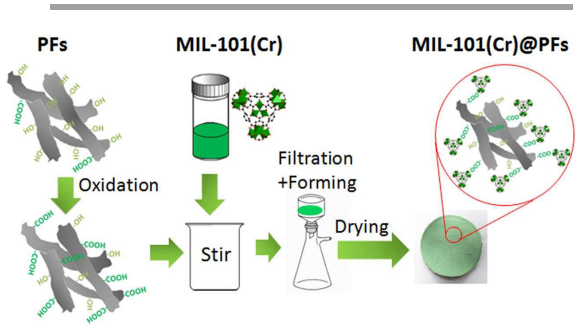

Fig. 1 Flow chart of preparation of the sheet composites MIL-101(Cr)@PFs of MIL-101(Cr) and the pulp fibers

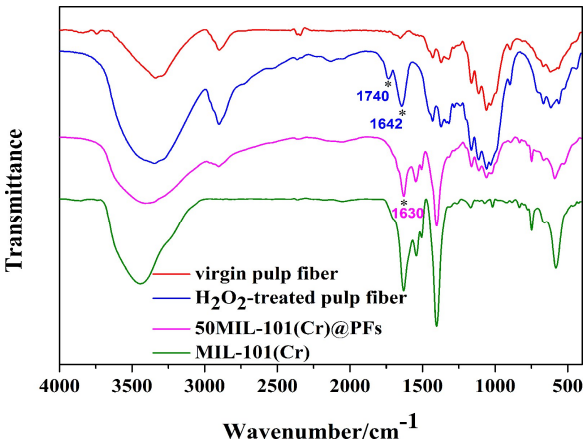

Fig. 3 FTIR spectra of the pulp fiber, MIL-101(Cr) and 50MIL-101(Cr)@PFs.

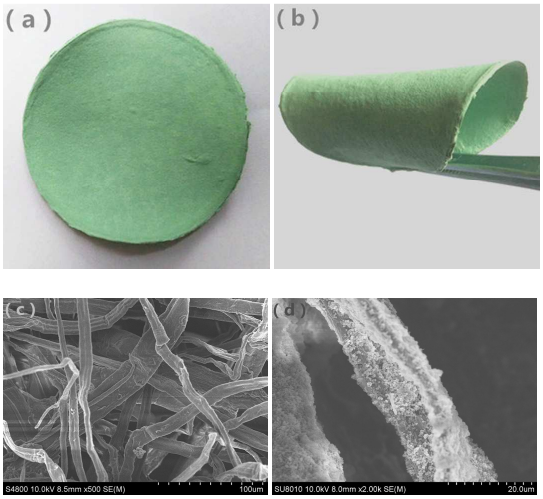

Fig. 2 Pictures of 50MIL-101(Cr)@PFs(a) and its flexibility performance(b); SEM image of virgin pulp fibers(c) and 50MIL-101(Cr)@PFs(d).

0.02°at range of 5-50°(2θ). Scanning electron microscope (SEM) data were obtained from a Hitachi S-4800 instrument, and samples were previously dried and the sample surfaces were gold metallized. FTIR spectroscopy was performed on a Bruker Vector 33 spectrometer with KBr pellets in the range of 4000–400 cm^{-1} with a resolution of 4 cm^{-1}. Before each measurement, the samples were evacuated at 423 K for 8 h. Thermal stability of samples were tested on a HTG-1/2 TGA in nitrogen atmosphere with the temperature range from 303K to 873K at a heating rate of 5 K/min.

2.5. Measurement of mechanical stability

Up to now, there are no uniform evaluation criteria for the mechanical stability of MOFs composites. Herein mechanical vibration test was designed to evaluate the mechanical stability of MIL-101(Cr)@PFs. Mechanical stability of composites MIL-101(Cr)@PFs was evaluated on a reciprocating oscillator (Fu Hua CHZ 82A) with adjustable oscillation frequency of 2 and 4 Hz at room temperature. In most situations of practical applications, the oscillation frequency does not exceed 2 Hz. Evaluation procedure was as follows: First, the sample MIL-101(Cr)@PFs was placed on the oscillator, and then exposed to air for enough time until there was no change in mass. After that, mechanical vibration test was carried out for 120 minutes, and the sample MIL-101(Cr)@PFs was weighed every 20 minutes during the measurements.

2.6. Measurement of benzene vapor and CO_2 adsorption isotherms

Adsorption isotherms of benzene vapor and CO_2 on MIL-101(Cr) and MIL-101(Cr)@PFs were separately measured at 298 K on the Micromeritics 3-Flex by using a standard static volumetric method. The temperatures were strictly controlled by using a Dewar with a circulating jacket connected to a thermostatic bath with a precision of ±0.01 K. The free space of the system was measured by dosing the helium gas (99.999%). Before each measurement, the samples were vacuumed and evacuated at 423 K for about 8 h. Measurement of CO_2 adsorption-desorption cycles also was performed on Micromeritics 3-Flex. MIL-101(Cr)@PFs were regenerated under vacuum and heated at 393 K for about 30 minutes after each adsorption.

3. Results and discussion

Fig.2 shows pictures of the as-synthesized MIL-101(Cr)@PFs and SEM images of virgin pulp fibers and MIL-101(Cr)@PFs. This sheet composite can be distorted up to 360° without damage, suggesting its excellent flexibility(Fig.2, Fig.S1). Fig.1(c-d) show MIL-101(Cr) crystals had been attached on surfaces of PFs, implying PFs were suitable substrates. Fig.S2 shows that the PXRD patterns for 50MIL-101(Cr)@PF. It exhibited the characteristic peaks at 2.95°, 3.40°, 5.25°, 8.55°, 9.15° and 16.58°, which were consistent with MIL-101(Cr) reported in the literature,[3, 13] indicating that MIL-101(Cr) crystals were immobilized on the pulp fibers without damage.

Fig.3 shows FTIR spectra of samples. Contrasting FTIR spectrum of original PF with that of H_2O_2-treated PF, we found that for H_2O_2-treated PF, its peak of the C=O at 1642 cm^{-1} was intensified,[34] and furthermore a new peak occurred at 1740 cm^{-1}, which were assigned to the vibration of carboxyl groups,[35] suggesting the production of carboxyl groups on PF after treated by hydrogen peroxide. It may be ascribed to the oxidation of hydroxyl groups on PF into carboxyl groups.[31] It was observed that MIL-101(Cr)@PFs retained the main characteristic peaks of both H_2O_2-treated PFs (the peaks occurred separately at 1031, 1113, and 2900 cm^{-1}) and parent MIL-101(Cr)(the peaks occurred separately at 582, 748, 1403, 1546 and 1630 cm^{-1}). However, it was noteworthy that after forming composite of MIL-101(Cr) and the H_2O_2-treated PF, the peak at 1740 cm^{-1} corresponding to carboxyl group on H_2O_2-treated PF disappeared on FTIR spectrum of MIL-101(Cr)@PFs, which may be ascribed to the chelation between Cr^{3+} and -COOH forming Cr-O bond. As a result, it resulted in the disappearance of vibration signal of carboxylic groups in IR spectrum. It implied that MIL-101(Cr) crystals had been anchored on the PFs. In addition, the peak reflecting C=O bond vibrations on the H_2O_2-treated PF at 1642 cm^{-1}

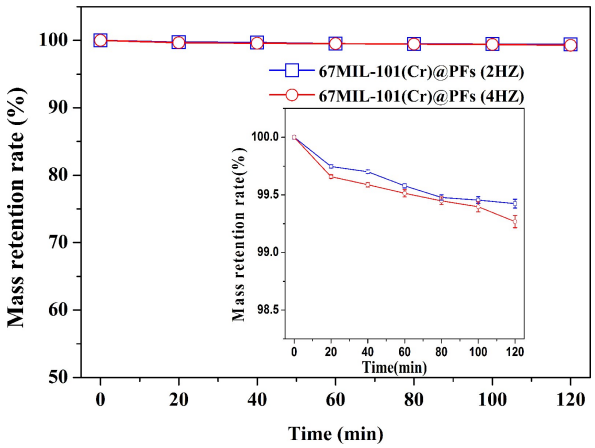

Fig. 4 Mechanical stability of 67MIL-101(Cr)@PFs evaluated by vibration experiment.

was shifted to lower wavenumbers and overlapped the peak of vas(COO) of the ionized carboxylate group on MIL-101(Cr)@PFs at 1630cm^{-1}.[36] This shirt can be ascribed to the coordination of electron-rich oxygen atoms of C=O bond on H_2O_2-treated PF to the electropositive transition metal cations Cr^{3+} on MIL-101(Cr),[30, 37] resulting in varied chemical environment after depositing MIL-101(Cr) on the H_2O_2-treated PFs.

In addition, a vibration experiment was designed to evaluate mechanical stability of the sheet composite. Fig.4 presents the mechanical stability of 67MIL-101(Cr)@PFs under condition of vibration at frequencies of 2HZ and 4HZ, respectively. To ensure the reliability of the data, we tested three samples of 67MIL-101(Cr)@PFs at the same time on the reciprocating oscillator at frequencies of 2HZ, and then we calculated the average values of three mass retention rate of each time(every 20 minutes). In addition, we also tested other three samples of 67MIL-101(Cr)@PFs at the same time on the reciprocating oscillator at frequencies of 4HZ. Figure 4 presents the average values of mass retention rates for 67MIL-101(Cr)@PFs at different frequencies.It showed that

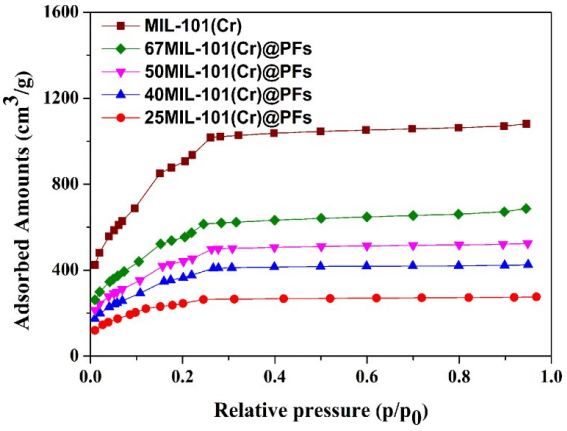

Fig. 5 N_2 adsorption isotherms of MIL-101(Cr) and MIL-101(Cr)@PFs at 77k

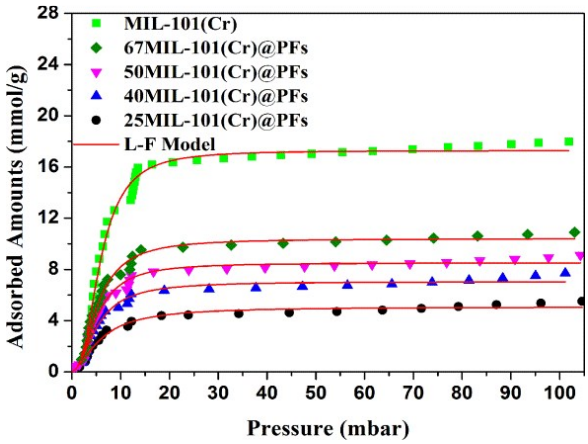

Fig. 6 Benzene vapor adsorption isotherms of MIL-101(Cr) and MIL-101(Cr)@PFs at 298 K.(Points, experimental data; solid curves, model fitting by L-F equation.)

mass retention rates of 67MIL-101(Cr)@PFs maintained up to 99.5% and 99.3% after vibration of 120 minutes at 2HZ and 4HZ, respectively, implying that MIL-101(Cr) crystals had been anchored on the pulp fibers, and thus the resulting sheet MIL-101(Cr)@PFs possessed excellent mechanical stability.

Fig.5 shows the N_2 isotherms of MIL-101(Cr)@PFs and MIL-101(Cr) at 77 K. These isotherms exhibited the typical type I profiles with secondary uptakes in the range of 0.14~0.25 (p/p_0), indicating the existence of two different microporous windows in all the samples.[3] The equilibrium amount adsorbed of N_2 on MIL-101(Cr)@PFs became lower compared to MIL-101(Cr) due to introduction of PFs, and it increased with the loading ratio of MIL-101 on the PFs. Table S1 lists the textural properties of MIL-101(Cr)@PFs. The surface area of MIL-101(Cr)@PFs increased with the loading ratio, reaching 2174 m^2/g at the loading ratio of 67%, about 65% of surface area of parent MIL-101(Cr).

Fig.S3 shows the pore size distribution of 50MIL-101(Cr)@PFs and MIL-101(Cr). It was clearly visible that the samples demonstrated similar pore size distribution with some difference in pore volume. Compared to MIL-101(Cr), the pore volume of 50MIL-101(Cr)@PFs became low due to introduction of nonporous PF substrate and similar phenomenon was reported by Rose[26] on HKUST-1 grown on PAN substrate.

Fig.S4 presents the SEM images of MIL-101(Cr), virgin pulp fibers and MIL-101(Cr)@PFs. It was observed that MIL-101(Cr) sample had good octahedral morphology, as shown in Fig. S4a, similar to that reported in the literature.[3] Fig.S4b shows the SEM image of virgin pulp fibers, exhibiting flexible structure of the pulp fibers. Fig.S4c presents the SEM image of MIL-101(Cr)@PFs. It was observed that MIL-101(Cr) crystals had been evenly dispersed and anchored on the pulp fibers. Fig.S5 presents TGA Curves of MIL-101(Cr)@PFs, MIL-101(Cr) and virgin pulp fiber. It was noticed that MIL-101(Cr)@PFs exhibited two significant weight drops, one starting at around 300 ℃, corresponding to the damages of PFs, and the other starting at around 350 ℃, corresponding to decomposition of MIL-101(Cr) crystals.[38] The TG analysis demonstrated the excellent thermal stability of MIL-101(Cr)@PFs.

Table 1 Comparison of benzene adsorption capacities on different adsorbents.

Adsorbent	Equilibrium adsorption capacity (mmol/g)	Temperature (K)	Reference
SBA-15	0.83	303	[13]
Silicalite-1	1	295	[13]
H-ZSM-5	1.3	303	[40]
Activated carbon	~7.5	303	[40]
ACC-963	4	303	[21]
HKUST-1	10	298	[21]
MOF-74	1.23	323	[41]
67MIL-101(Cr)@PFs	10.29	298	This work
MIL-101(Cr)	16.54	298	This work

Fig.6 shows the isotherms of benzene vapor on MIL-101(Cr)@PFs and the parent MIL-101(Cr). It can be seen that the equilibrium amounts adsorbed of benzene on these composites increased with the percentage of MIL-101(Cr) loaded on the PFs. These isotherms exhibited typical type I curves with second adsorptions in pressure range of 8 to 15 mbar due to the presence of two kinds of pore windows in the samples.[39] The benzene uptake increased rapidly with pressure at low pressure region (P <15 mbar), which can be attributed to the strong adsorption of benzene on the unsaturated metal centers and the micropore of MIL-101(Cr).[13, 21] Table S2 lists the benzene uptakes of MIL-101(Cr) and MIL-101(Cr)@PFs. Thereinto, the benzene uptake of 67MIL-101(Cr)@PFs reached 10.29 mmol/g, being 62% of that (16.54 mmol/g) of parent MIL-101(Cr) at 298K and 25 mbar, suggesting that the coating process had less impact on the adsorption performance of MIL-101(Cr) crytals.

For comparison, Table 1 presents the benzene adsorption capacities of different adsorbents. The data in Table 1 indicated that the benzene equilibrium adsorption capacity of 67MIL-101(Cr)@PFs achieved 10.29 mmo/g, much higher than those of conventional adsorbents. For example, the equilibrium adsorption capacity of 67MIL-101(Cr)@PFs for benzene was 12 times, 10 times, and 7.7 times as much as that of the SBA-15, Silicalite-1, H-ZSM-5, respectively. Furthermore, it was also higher than those of many metal organic frameworks such as HKUST-1, UIO-66 and MIL-100(Cr). Therefore, 67MIL-101(Cr)@PFs will be a promising adsorbent for practical application of VOCs capture.

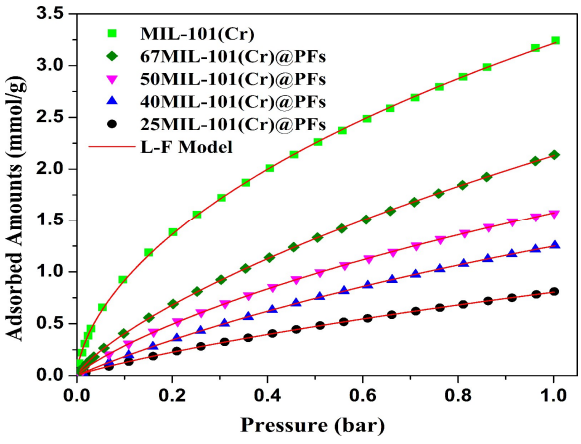

Fig. 7 CO_2 isotherms of MIL-101(Cr) and MIL-101(Cr)@PFs at 298 K.(Points, experimental data; solid curves, model fitting by L-F equation.)

Fig.7 presents the isotherms of CO_2 on MIL-101(Cr)@PFs. It showed that the CO_2 equilibrium uptakes of MIL-101(Cr)@PFs increased with the percentage of MIL-101(Cr) loadings, and thus that of 67 MIL-101(Cr)@PFs reached 2.13 mmol/g at 298 K and 1 bar. Table S2 lists the CO_2 adsorption capacities of MIL-101(Cr) and MIL-101(Cr)@PFs at 298 k and 1 bar. It was noted that that the CO_2 uptakes of MIL-101(Cr)@PFs were proportional to the amounts loaded of MIL-101(Cr) on the PFs, almost equivalent to the CO_2 uptake of MIL-101(Cr) loaded on the PFs. For example, 67MIL-101(Cr)@PF demonstrated an CO_2 uptake of 2.13 mmol/g, reaching 65.7% as much as that of parent MIL-101(Cr). It suggested that MIL-101(Cr) crystals loaded on the MIL-101(Cr)@PFs keep their unsaturated metal sites Cr(III) capable of capturing CO_2 by Lewis acid-base interactions between the O of CO_2 and Cr(III).[42] It further indicated that the MIL-101(Cr) crystals loaded on the PFs still maintained their adsorption performance after the deposition and molding processes. Table S3 presents a comparison of CO_2 adsorption capacities of different adsorbents. It showed that 67MIL-101(Cr)@PFs demonstrated a more excellent CO_2 uptake of 2.13 mmol/g in comparison to conventional adsorbents such as ZSM-5, zeolite-13X, MCM-41 and AC. Furthermore, it was worthy of mentioning that CO_2 adsorption capacity of 67MIL-101(Cr)@PFs was higher than those of some MOFs crystals including ZIF-68, UIO-66 and MOF-5.

In order to describe the adsorption of benzene and CO_2 on the MIL-101(Cr)@PFs quantificationally, the Langmuir–Freundlich (L–F) equation was applied to fit the experimental isotherm data of benzene and CO_2, as shown in Fig.6 and Fig.7. L–F equation can be expressed as follows:

$$Q = q\frac{bp^c}{1+bp^c} \qquad (1)$$

Where, p (mbar or bar) is the pressure of the gas at equilibrium state; Q is the equilibrium uptake; q (mmol/g) is the saturation adsorption capacities; b ($mbar^{-1}$ or bar^{-1}) is the equilibrium constant of adsorption; c is the Langmuir–Freundlich coefficient.

Table S4 and S5 list the fitting parameters of L-F model as well as their correlation coefficients (R^2) for linear regression of data of benzene and CO_2 adsorption on the samples MIL-101(Cr) and MIL-101(Cr)@PFs at 298 K separately. The high regression coefficient R^2 up to 0.975 indicated that the L-F model gave a good fit to the experimental isotherms of benzene and CO_2 on the samples.

Figure S6 presents CO_2 isotherms of each cycle of adsorption-desorption on 50MIL-101(Cr)@PFs. These CO_2 isotherms were nearly overlapping. The regeneration efficiency of 50MIL-101(Cr)@PFs was up to 99% as shown in Figure S7, suggesting that 50MIL-101(Cr)@PFs had excellent regeneration property. Thus, it can be concluded that CO_2 adsorption on MIL-101(Cr)@PFs was stable and reversible.

Conclusions

In summary, an novel method of immobilizing MIL-101(Cr) crystals on PFs was successfully developed for preparing sheet MIL-101(Cr)@PFs. The as-prepared MIL-101(Cr)@PFs were flexible, which can be distorted up to 360° without damage. More importantly, mass retention rates of 67MIL-101(Cr)@PFs maintained up to 99.5% and 99.3% after vibration of 120 minutes at 2HZ and 4HZ, respectively, suggesting the sheet composite is very stable. The surface area of MIL-101(Cr)@PFs increased with the amount loaded of MIL-101(Cr) crystals on the PFs, which can reach 2174 m^2/g when the amount loaded was of 67%. The benzene and CO_2 uptake of 67MIL-101(Cr)@PFs reached 10.29 mmol/g(298K, 25 mbar) and 2.13 mmol/g(298K, 1bar), respectively. Its adsorption performance is much better than many traditional adsorption materials. Its excellent flexibility and mechanical stability can make the composites be manufactured into various shapes to meet the different requirements of practical applications. It can be expected that the sheet MIL-101(Cr)@PFs would become a promising adsorption material for gas adsorption and purification, such as CO_2 and VOCs as well as toxic gases, in practical applications. In addition, the forming method of MOFs@PFs would be an effective way to prepare catalystic materials for gas purification purposes.

Acknowledgements

This work was supported by National Key Basic Research Program of China (2013CB733506), National Natural Science Foundation of China (No.51276065; No. 21436005), the Guangdong Natural Science Foundation (No. 2014A030312007), and the Research Foundation of State Key Lab of Subtropical Building Science of China (C715023z).

Notes and references

1. Q. L. Zhu and Q. Xu, *Chemical Society reviews*, 2014, **43**, 5468-5512.
2. S. Li and F. Huo, *Nanoscale*, 2015, **7**, 7482-7501.
3. X. Sun, Q. Xia, Z. Zhao, Y. Li and Z. Li, *Chemical Engineering Journal*, 2014, **239**, 226-232.
4. X. Zhou, W. Huang, J. Miao, Q. Xia, Z. Zhang, H. Wang and Z. Li, *Chemical Engineering Journal*, 2015, **266**, 339-344.
5. K. K. Tanabe and S. M. Cohen, *Chemical Society reviews*, 2011, **40**, 498-519.
6. J. Lee, O. K. Farha, J. Roberts, K. A. Scheidt, S. T. Nguyen and J. T. Hupp, *Chemical Society reviews*, 2009, **38**, 1450-1459.
7. E. V. Ramos-Fernandez, M. Garcia-Domingos, J. Juan-Alcañiz, J. Gascon and F. Kapteijn, *Applied Catalysis A: General*, 2011, **391**, 261-267.
8. W. Qin, W. Cao, H. Liu, Z. Li and Y. Li, *RSC Adv.*, 2014, **4**, 2414-2420.
9. L. J. Murray, M. Dinca and J. R. Long, *Chemical Society reviews*, 2009, **38**, 1294-1314.
10. R. Sathre and E. Masanet, *RSC Adv.*, 2013, **3**, 4964-4975.
11. Z. Zhang, Y. Zhao, Q. Gong, Z. Li and J. Li, *Chemical Communications*, 2013, **49**, 653-661.
12. J. Liu, P. K. Thallapally, B. P. McGrail, D. R. Brown and J. Liu, *Chemical Society reviews*, 2012, **41**, 2308-2322.
13. S. Xian, Y. Yu, J. Xiao, Z. Zhang, Q. Xia, H. Wang and Z. Li, *RSC Adv.*, 2015, **5**, 1827-1834.
14. R.-L. Tseng, F.-C. Wu and R.-S. Juang, *Separation and Purification Technology*, 2015, **140**, 53-60.
15. K. Nieszporek, M. Drach and P. Podkościelny, *Separation and Purification Technology*, 2009, **69**, 174-184.
16. Y. Lee, D. Liu, D. Seoung, Z. Liu, C.-C. Kao and T. Vogt, *Journal of the American chemical society*, 2011, **133**, 1674-1677.
17. A. Möller, A. P. Guimaraes, R. Gläser and R. Staudt, *Microporous Mesoporous Mat.*, 2009, **125**, 23-29.
18. M. Ncube and Y. Su, *International Journal of Sustainable Built Environment*, 2012, **1**, 259-268.
19. A. R. Millward and O. M. Yaghi, *Journal of the American Chemical Society*, 2005, **127**, 17998-17999.
20. P. Li, J. Chen, W. Feng and X. Wang, *Journal of the Iranian Chemical Society*, 2013, **11**, 741-749.
21. Z. Zhao, S. Wang, Y. Yang, X. Li, J. Li and Z. Li, *Chemical Engineering Journal*, 2015, **259**, 79-89.
22. F. Jeremias, D. Fröhlich, C. Janiak and S. K. Henninger, *New Journal of Chemistry*, 2014, **38**, 1846-1852.
23. X. Zhou, W. Huang, J. Shi, Z. Zhao, Q. Xia, Y. Li, H. Wang and Z. Li, *Journal of Materials Chemistry A*, 2014, **2**, 4722.
24. D. Farrusseng, S. Aguado and C. Pinel, *Angewandte Chemie International Edition*, 2009, **48**, 7502-7513.
25. P. Küsgens, S. Siegle and S. Kaskel, *Advanced Engineering Materials*, 2009, **11**, 93-95.
26. M. Rose, B. Böhringer, M. Jolly, R. Fischer and S. Kaskel, *Advanced Engineering Materials*, 2011, **13**, 356-360.
27. J. Gascon, M. D. Hernández‐Alonso, A. R. Almeida, G. P. van Klink, F. Kapteijn and G. Mul, *ChemSusChem*, 2008, **1**, 981-983.
28. M. G. Schwab, I. Senkovska, M. Rose, M. Koch, J. Pahnke, G. Jonschker and S. Kaskel, *Advanced Engineering Materials*, 2008, **10**, 1151-1155.
29. M. da Silva Pinto, C. A. Sierra-Avila and J. P. Hinestroza, *Cellulose*, 2012, **19**, 1771-1779.
30. A. R. Abbasi, K. Akhbari and A. Morsali, *Ultrasonics sonochemistry*, 2012, **19**, 846-852.
31. B. Wang, M. Li, Q. Zhao, Y. Qin and K. Xie, *JOURNAL OF CHEMICAL INDUSTRY AND ENGINEERING-CHINA-*, 2004, **55**, 1329-1334.
32. K. S. Walton and R. Q. Snurr, *Journal of the American Chemical Society*, 2007, **129**, 8552-8556.
33. J. Peng, S. Xian, J. Xiao, Y. Huang, Q. Xia, H. Wang and Z. Li, *Chemical Engineering Journal*, 2015, **270**, 282-289.
34. P. D. Nallathamby, N. P. Mortensen, H. A. Palko, M. Malfatti, C. Smith, J. Sonnett, M. J. Doktycz, B. Gu, R. K. Roeder, W. Wang and S. T. Retterer, *Nanoscale*, 2015, **7**, 6545-6555.
35. Y. Xue, Z. Wang, J. Wang, C. Hu, F. Xie, D. Chen and Z. He, *ISRN Spectroscopy*, 2012, **2012**, 1-6.
36. B. L. Liu, J. Dang, S. Q. Zang, Q. L. Wang and R. J. Tao, *Zeitschrift für Naturforschung B*, 2010, **65**, 1240-1244.
37. A. R. Abbasi and A. Morsali, *Ultrasonics sonochemistry*, 2011, **18**, 282-287.
38. Y. Lin, H. Lin, H. Wang, Y. Suo, B. Li, C. Kong and L. Chen, *Journal of Materials Chemistry A*, 2014, **2**, 14658-14665.
39. X. J. Sun, Y. J. Li, H. X. Xi and Q. B. Xia, *RSC Adv.*, 2014, **4**, 56216-56223.
40. S. H. Jhung, J. H. Lee, J. W. Yoon, C. Serre, G. Férey and J. S. Chang, *Advanced Materials*, 2007, **19**, 121-124.

41. D. Britt, D. Tranchemontagne and O. M. Yaghi, *Proceedings of the National Academy of Sciences*, 2008, **105**, 11623- 11627.
42. Q. Liu, L. Ning, S. Zheng, M. Tao, Y. Shi and Y. He, *Scientific reports*, 2013, **3**, 2916.